

Part II - Hydraulic design of embankment overflow stepped spillways

7. Embankment overflow stepped spillways

Flood protection of an embankment dam is usually achieved by combining a side spillway of relatively large capacity with a reservoir storage "buffer" (i.e. empty volume) for flood attenuation. In recent years, the design floods of a number of dams were re-evaluated and the revised flows were often larger than those used for the original designs. In many cases, occurrence of the revised design floods would result in dam overtopping because of the insufficient storage and spillway capacity of the existing reservoir. Embankment overtopping is not acceptable because the rushing waters would scour the embankment slope leading to the rapid and total failure of the embankment.

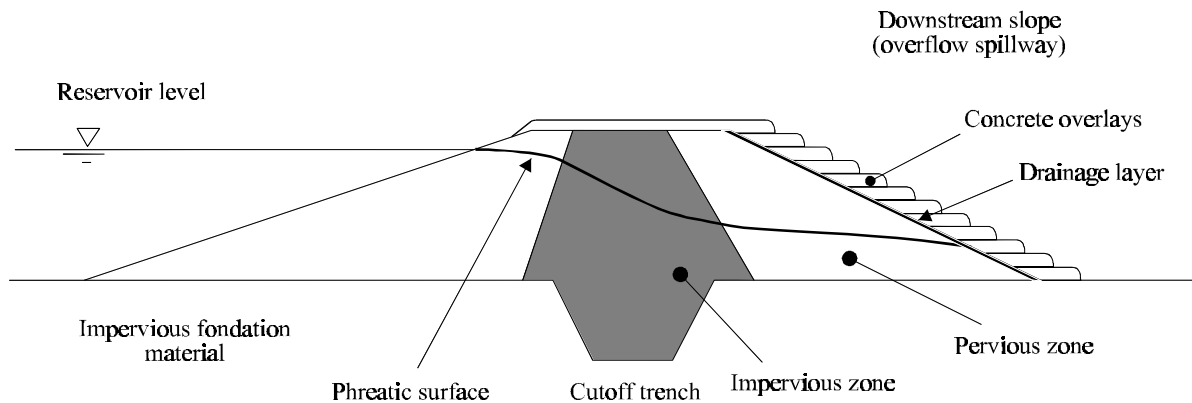
Some overflow systems were developed in Australia : e.g., flow through rockfill embankment (e.g. OLIVIER 1967), the minimum energy loss weir design (e.g. Chinchilla weir, TURNBULL and McKAY 1974), the concrete slab chute system at Crotty rockfill dam (Tasmania). Although technically successful, these designs are not often economical. Recently new flood protection systems were introduced, allowing controlled embankment overtopping over a reinforced downstream stepped slope. Basic reinforcement techniques include concrete overtopping protection, precast concrete blocks, timber cribs, sheet-piles, riprap and gabions, and reinforced earth.

Concrete overtopping protection

Concrete overtopping protection allows an increase of spillway capacity. In North-America, a number of dam overtopping rehabilitations were conducted primarily on embankment structures with dam heights ranging from 4.6 to 33.5 m. It is believed that the first ones were the Ocoee No. 2 timber crib dam in 1980 and the Brownwood Country Club earth dam in 1984. Various construction techniques were used. Current trends favour the use of roller compacted concrete (RCC) ⁽⁷⁾ (Fig. 7-1).

⁷RCC dam rehabilitation accounted for nearly two-thirds of the RCC dam construction in USA in the 1990s.

Fig. 7-1 - Concrete overflow protection system for embankments
(A) Sketch of an overflow protection system with roller compacted concrete



(B) Construction of a RCC spillway for detention basin West of Las Vegas, designed by the US Corps of Engineers



Roller compacted concrete is placed in a succession of overlays of 0.2 to 0.4-m thickness and with a width greater than 2.5 m for proper hauling, spreading and compacting. Exposed RCC is frequently used for secondary spillways with infrequent spills of less than 5 m²/s. Alternatively, a conventional concrete protection overlay may be applied after the RCC or at the completion of construction works to

protect the RCC. With both RCC and conventional concrete protection, a drainage system beneath the concrete layers is essential to prevent uplift. Its purpose is to relieve pore pressure at the interface between the embankment and RCC overlays. In some cases, the drainage installation may be replaced or supplemented with drain holes formed through the RCC during placement. At the downstream end a cutoff wall must be built to prevent undermining of the concrete layer during overtopping.

Precast concrete steps

Soviet engineers were among the first to propose a stepped concrete chute design on the downstream face of embankment dams under the leadership of P.I. GORDIENKO (CHANSON 1995a, 2001) (Fig. 7-2). The choice of a stepped structure allows the use of individual blocks interlocked with the next elements and the design assists in the energy dissipation. The design concept was more recently tested in USA and UK, although it did not prove cost-effective there. An interesting feature of the concrete block system is the flexibility of the stepped channel bed allowing differential settlements of the embankment.

Fig. 7-2 - Earth dam stepped spillway with precast concrete blocks : Sosnovsky farm dam (Russia, 1980) (Courtesy of Prof. Y. PRAVDIVETS) - $H = 11$ m, design flow : $3.3 \text{ m}^2/\text{s}$, $\alpha = 10^\circ$, $W = 12$ m, overlapping precast concrete blocks ($1.5 \text{ m} \times 3 \text{ m} \times 0.16 \text{ m}$)



Fig. 7-3 - Earthfill embankment with a rockfill upstream protection and reinforced earth downstream slope construction : Jordan II, Gatton QLD (Australia, 1992) on 22 Feb. 1998 - H = 5.3 m, h = 1.4 m, $\alpha = 17.7^\circ$ - View from downstream



For an earth dam with overflow precast block stepped spillway, the most important criterion is the stability of the dam material. Seepage may occur in a saturated embankment and the resulting uplift pressures can damage or destroy the stepped channel and the dam : adequate drainage is essential. In a typical design, the blocks lay on a filter and erosion protection layer. The layer has the functions of filtering the seepage flow out of the subsoil and protecting the subsoil layer from erosion by flow in the drainage layer. The protection layer reduces or eliminates the uplift pressures acting on the concrete blocks. Usually a geotextile membrane is laid on the embankment before the placing of the layer, and another covers the protection layer before the installation of the blocks.

There is a basic design rule for precast concrete block systems : a skimming flow in a straight prismatic chute. The step block system was developed for a skimming flow regime : i.e., maximum block stability can only be achieved in skimming flows (e.g. BAKER 2000).

Alternatives for embankment stepped overflow

Alternative overtopping protection systems include timber cribs, sheet-piles, riprap and gabions, and reinforced earth. Timber crib overflows were used as early as the 18th century in Russia and some recent structures are still in use in Australia (CHANSON 2001). A number of weirs were designed with

steel sheet-piles and concrete slabs in Russia and Australia. An experimental structure was built with a reinforced-earth stepped overflow (Fig. 7-3). Another alternative is an overflow system made with gabions and Reno mattresses (e.g. CHANSON 1995a).

8. Hydraulic design of embankment overflow stepped spillways

8.1 Presentation

The design of embankment overflow stepped spillway is a critical issue. Any single failure of the spillway system can lead to a total dam failure. The professional community lacks basic design guidelines and current expertise is empirical.

For the design of an embankment overflow stepped spillway, a number of specific key issues must be assessed accurately and this includes :

[1] Stepped spillway operation and chute erosion

The stepped chute is designed to dissipate safely some kinetic energy, without damage to the steps. The spillway flow conditions cannot be calculated as for conventional flat (smooth invert) chutes.

[2] Embankment seepage

Seepage takes place in the embankment for high reservoir water levels. Strong interactions may occur between the free-surface flow and seepage flow in the embankment, that could cause uplift pressures leading to the destruction of the spillway, hence of the dam.

[3] Drainage beneath steps

A drainage system beneath the concrete steps is essential to prevent build-up of uplift pressures. Its purpose is to relieve pore pressure at the interface between the embankment and concrete steps. (Two stepped block spillways failed in Russia because of inadequate drainage layer (CHANSON 2000b).)

[4] Sidewalls (overtopping, scour)

The chute and crest sidewalls must be designed to prevent any overtopping for all flow rates up to PMF. The design of chute sidewalls must take into account the flow bulking resulting from the free-surface aeration. If splashing is acceptable, the training wall height may be sized to contain the characteristic air-water depth Y_{90} for all flow rates up to design flows. If the surroundings (e.g. embankment) are at risk of erosion, the sidewall height must be designed for $1.4*Y_{90}$. When the

developing spray can lead to fog or ice on surrounding roads or settlements, a greater safety margin must be considered. Note that the calculations of sidewall heights depend upon the type of flow regime (nappe, transition, skimming flow regimes).

Further strong secondary currents exist at the connection between the steps and the abutment walls. These are associated with high risks of scour, and the connections steps/abutment must be reinforced adequately.

[5] Sidewalls (chute convergence effects)

When the overflow spillway extends across the entire dam crest (e.g. Melton dam, Australia), the topography of the valley induces a convergence of the overflow. While a slight chute convergence may not affect the overall flow patterns, a reduction in channel width causes a modification of the discharge per unit width q_w and possibly a change in flow regime. Flow conditions at transition between flow regime could exhibit some instabilities leading to deflecting nappes and fluctuating hydrodynamic loads on the steps.

In nappe and skimming flows, sidewall convergence may further cause free-surface instabilities, including shock waves, flow concentrations, secondary currents and sidewall splashing that may be unacceptable.

[6] Downstream energy dissipation and scour

At the downstream end of the stepped chute, further energy dissipation takes place beneath the hydraulic jump or in the plunge pool for high tailwater levels. Turbulent fluctuations (velocity and pressure) in the hydraulic jump and at the plunge point may cause damage to the chute toe and sidewalls.

8.2 Discussion

Secondary currents at the connection between steps and (smooth) abutment walls

At the connection between the steps and the abutment walls ⁽⁸⁾, the differences in flow resistance between stepped invert and smooth concrete abutment generate transverse velocity gradient. Strong secondary currents associated with high shear forces develop and the risks of scour are high.

⁸This is especially important when the abutment is not a vertical concrete wall.

Major scour at abutments was observed during a number of flood events above overflow stepped weirs in Queensland : e.g., Whetstone weir (1953 overflow), Bonshaw weir (1956 failure) (CHANSON 2000b). In a keynote lecture on stepped block spillways, Dr BAKER emphasised that a known construction weakness is the joint between the chute invert and the sidewalls (BAKER 2000). (At Brushes Clough stepped spillway (UK), two longitudinal concrete guides were built to facilitate the installation of the blocks and the connection with the stone-pitched sidewalls.)

Chute convergence

To date, nearly all bibliography on stepped chute hydraulics applies to prismatic rectangular channels. Literature on converging stepped chutes is rare, but for TALBOT et al. (1997).

In nappe and skimming flows, sidewall convergence may cause shock waves propagating across the chute and impacting onto the opposite chute walls. At Gold Creek dam stepped spillway (Australia), significant flow disturbances and sidewall splashing caused by shock waves was observed during a 1996 overflow (CHANSON and WHITMORE 1998). Shock waves cause further flow concentrations and induce three-dimensional instabilities that may not be acceptable (CHANSON 2001, chap. 9).

Interactions between seepage and free-surface flows

During overflows, seepage takes place in the embankment. It is influenced by the infiltration into the downstream slope caused by the spillway flow, in addition to the flow through the embankment itself. Appropriate provision for drainage and evacuation of seepage flow through the steps is required. Drains are usually installed on the vertical face of the steps (Fig. 7-2, 8-1).

In skimming flows, the seepage that is drained into the step cavity may affect the cavity recirculation and in turn the turbulent dissipation process. It may lead to a reduction in flow resistance and an increase of the flow velocity at the downstream of the chute (i.e. at the plunge point, hydraulic jump or ski jump).

Flow resistance in skimming flows is a form drag mechanism predominantly (RAJARATNAM 1990, CHANSON et al. 2000). With form drag, fluid injection in the separated region (i.e. the cavity) does reduce drastically the drag (e.g. WOOD 1964, NAUDASCHER and ROCKWELL 1994). Table 8-1 summarises well-known studies, illustrated in Figure 8-2. A related case is the flow above a porous sill.

The writers hypothesise that a similar mechanism may exist in skimming flows above embankment stepped spillway. Note that this drag reduction mechanism differs and may add to drag reduction induced by free-surface aeration (see Paragraph 6.3).

Fig. 8-1 - Interactions between seepage flow and cavity recirculation

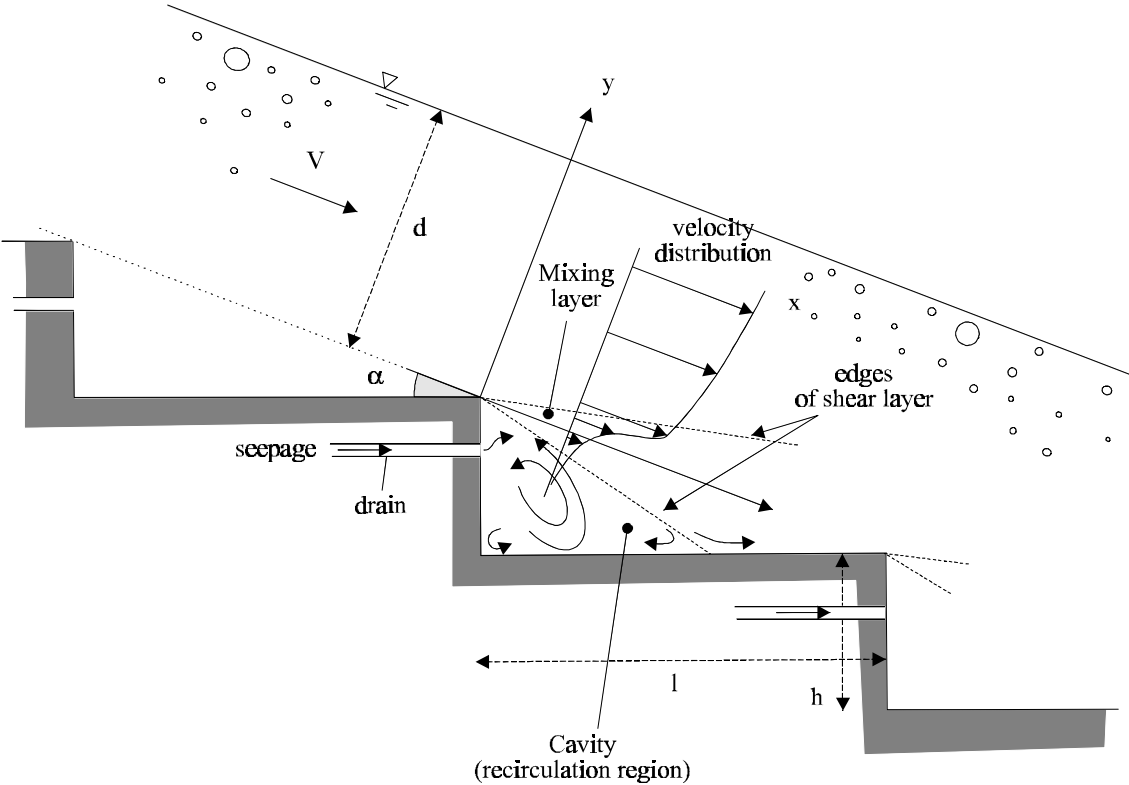
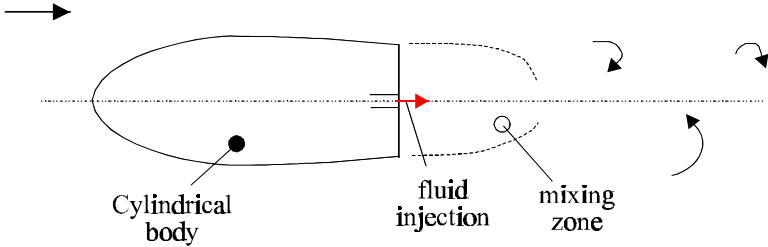
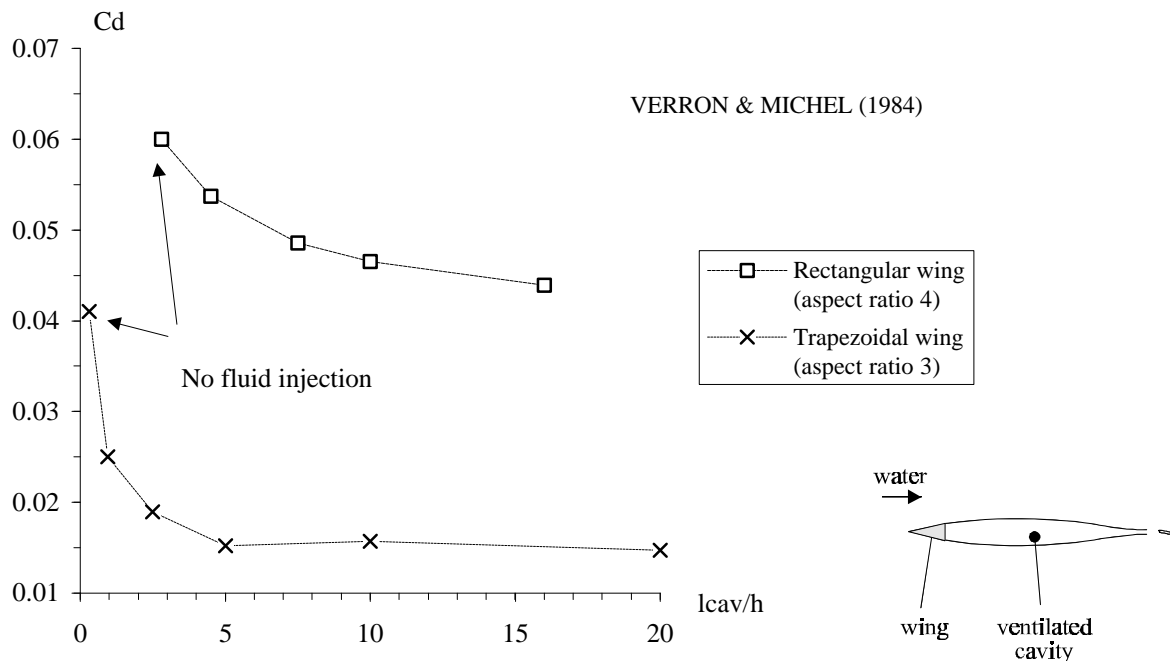


Figure 8-2 - Drag reduction behind bluff body associated with fluid injection
 (A) Sketch of WOOD's (1964) experiments



(B) Drag coefficient C_d on ventilated wings as a function of the dimensionless cavity length l_{cav}/h which is a function (VERRON and MICHEL 1984)



Downstream energy dissipation in a plunge pool

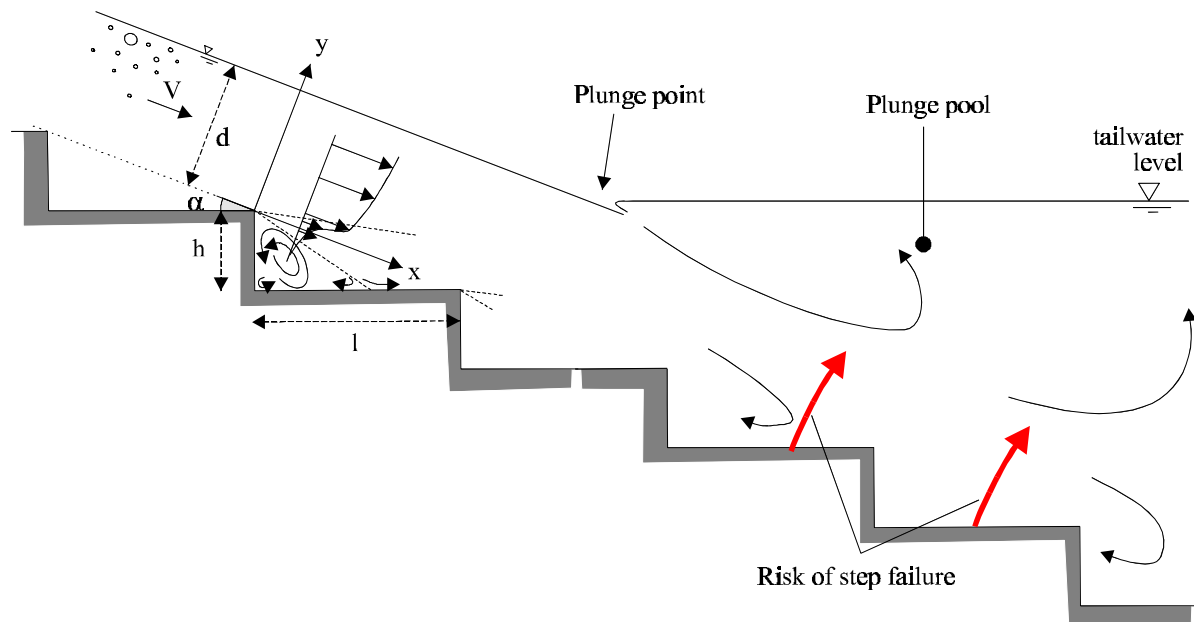
At the downstream end of the spillway, energy dissipation is usually achieved by (1) a high velocity water jet taking off from a flip bucket and impinging into a downstream plunge pool acting as a water cushion (e.g. Sosnovsky farm dam, Fig. 7-2), (2) a standard stilling basin downstream of the spillway where a hydraulic jump is created to dissipate a large amount of flow energy (e.g. U.S. Bureau of Reclamation designs), or (3) a plunge pool for high tailwater levels. In the latter case, the stability of the steps immediately beneath the plunge point (i.e. below tailwater level) is at risk (Fig. 8-3). Potential scour of the submerged steps is an issue that should be investigated in details with physical modelling.

BAKER (2000) observed major damage to stepped block spillway sections submerged by a hydraulic jump and a plunge pool. He illustrated his keynote lecture with an audio-visual documentary. YASUDA and OHTSU (2000) investigated the characteristics in the plunge pool downstream of a stepped chute as a function of the tailwater level. Although their results did not include efforts on the submerged steps, they observed some energy dissipation contribution from the submerged steps, suggesting some loads on the steps. The writers believe that this mode of failure is the worst for embankment overflow stepped spillways.

Table 8-1 - Drag reduction induced by fluid injection behind a bluff body

Reference (1)	Flow situations (2)	Description (3)
Fluid injection		
WOOD (1964)	Air flow past aerofoil with base bleed.	Drag reduction by fluid injection. Up to 60% drag reduction.
ABDUL-KHADER and RAI (1980)	Open channel flow past bridge piers ($0.2 < Fr < 0.65$).	Drag reduction with slotted piers. Up to 50% drag reduction.
SURYANARAYANA et al. (1993), SURYANARAYANA and PRABHU (2000)	Wind flow past a sphere.	Drag reduction by ventilation of the wake. Up to 60% drag reduction.
Cavity ventilation		
MICHEL and ROWE (1974)	Water flow past hydrofoil wings. Air ventilation.	Drag reduction with air ventilation at downstream end. Up to 83% drag reduction.
VERRON and MICHEL (1984)	Water flow past hydrofoil wings (rectangular and trapezoidal). Air ventilation	Drag reduction with air ventilation behind the wings. Up to 65% drag reduction.
Porous bluff body		
COOK (1990)	Wind flow past porous fences.	Drag reduction with increasing porosity : $Drag \propto (1 - C^2)$, C being the porosity.

Fig. 8-3 - Flow patterns at the plunge point



9. Conclusion

New experiments were conducted in a large-size stepped chute (1V:2.5H, $h = 0.1$ m, $W = 1$ m). Visual observations demonstrated three types of flow regimes : nappe flow, transition flow and skimming flow. The transition flow regime was observed for a relatively broad range of flow rates. It was characterised by a chaotic flow motion, strong splashing and very significant aeration.

Detailed air-water flow measurements were conducted in both transition and skimming flows immediately downstream of the inception point of free-surface aeration. In skimming flows, a complete characterisation was developed for the distributions of void fraction, bubble count rate and velocity. Although the air concentration distribution has the same shape as smooth chute flows, a slightly different trend was consistently observed, associated with strong droplet ejections. Flow resistance data are consistent with re-analysed data obtained in large-size laboratory chutes (Fig. 6-2). The re-analysis of all data highlights three dominant values of Darcy friction factor that are hypothesised to be three different modes of excitation. Drag reduction caused free-surface aeration was observed (Eq. (6-4), Fig. 6-5). It is believed to be caused by interactions between small entrained bubbles and developing mixing layers at each step edge.

Transition flows exhibited significantly different air-water flow properties from those observed in skimming flows. For each experiment, a deflected nappe was observed occasionally (i.e. at one step). The deflected jet was highly aerated and the associated spray would overtop the 1.25 m high sidewall. Although the study was limited to one slope and for a short canal, the results highlighted the complexity of the free-surface aeration down stepped cascades.

For ancient embankments and new earthfill dams, an overflow stepped spillway may be considered as a main flood release structure. A number of design alternatives exists : concrete protection layer, precast concrete blocks, timber cribs, gabions. The hydraulic design of such stepped spillways includes a number of specific aspects which must be taken into account, including seepage beneath the steps, interactions between seepage and free-surface flows, and downstream energy dissipation in plunge pool for high tailwater levels. Step stability below the plunge point is probably the worst loading scenario for high tailwater levels and it must be investigated with a physical model in absence of experimental data.

It is believed that embankment overflow stepped spillways have a number of specific features that must be considered carefully, and that further experimental works is required to understand the interactions

between seepage and free-surface flows.

Acknowledgements

The writers thank Dr John MACINTOSH, Water Solutions, for his detailed review and comments. They acknowledge the assistance of M. EASTMAN, N. VAN SCHAGEN, and G. ILLIDGE (The University of Queensland). The first author thanks Professor APELT, Dr MATOS, Professor OHTSU, Dr ROYET, and Dr YASUDA for helpful discussions and for providing their experimental data.

Appendix I - Summary of experimental results

Tableau I-1 - Single-tip conductivity probe data (Series 1)

Q_w m ³ /s	Location	$\frac{Y_{90}}{d_c}$	C_{mean}	$\frac{(F_{ab})_{max} * d_c}{V_c}$	$\frac{U_w}{V_c}$
(1)	(2)	(3)	(4)	(5)	(6)
Series 1					
0.1819	Step edge 6	0.44	0.15	4.30	2.64
0.1819	Step edge 7	0.52	0.24	7.59	2.55
0.1819	Step edge 8	0.51	0.28	13.38	2.71
0.164	Step edge 6	0.45	0.16	5.24	2.64
0.164	Step edge 7	0.55	0.31	9.79	2.62
0.164	Step edge 8	0.53	0.29	15.45	2.66
0.1467	Step edge 5	0.44	0.13	3.50	2.60
0.1467	Step edge 6	0.49	0.24	8.68	2.69
0.1467	Step edge 7	0.59	0.36	12.96	2.63
0.1467	Step edge 8	0.59	0.34	16.98	2.56
0.1301	Step edge 5	0.44	0.15	3.52	2.68
0.1301	Step edge 6	0.52	0.27	9.48	2.64
0.1301	Step edge 7	0.65	0.42	15.37	2.65
0.1301	Step edge 8	0.60	0.35	18.39	2.56
0.1237	Step edge 5	0.46	0.19	5.30	2.71
0.1237	Step edge 6	0.54	0.32	13.21	2.74
0.1237	Step edge 7	0.69	0.41	15.91	2.48
0.1237	Step edge 8	0.61	0.36	18.57	2.58
0.1142	Step edge 5	0.46	0.22	5.16	2.76
0.1142	Step edge 6	0.56	0.36	13.07	2.79
0.1142	Step edge 7	0.76	0.43	16.37	2.31
0.1142	Step edge 8	0.63	0.36	19.43	2.47
0.103	Step edge 4	0.44	0.14	2.85	2.67
0.103	Step edge 5	0.54	0.28	7.34	2.56
0.103	Step edge 6	0.68	0.46	14.33	2.70
0.103	Step edge 7	0.76	0.48	15.29	2.51
0.103	Step edge 8	0.57	0.34	18.63	2.65
0.099	Step edge 4	0.43	0.13	2.87	2.64
0.099	Step edge 5	0.56	0.33	8.52	2.66
0.099	Step edge 6	0.75	0.52	13.77	2.77
0.099	Step edge 7	0.63	0.35	16.97	2.46
0.099	Step edge 8	0.62	0.43	18.69	2.80
0.0845	Step edge 4	0.49	0.22	4.05	2.63
0.0845	Step edge 5	0.76	0.53	10.04	2.81
0.0845	Step edge 6	0.64	0.44	14.49	2.79
0.0845	Step edge 7	0.69	0.46	15.10	2.68
0.0845	Step edge 8	0.62	0.43	17.68	2.83
0.0799	Step edge 4	0.55	0.30	4.59	2.60
0.0799	Step edge 5	0.85	0.56	10.14	2.65
0.0799	Step edge 6	0.67	0.39	13.61	2.45
0.0799	Step edge 7	0.73	0.44	15.42	2.44
0.0799	Step edge 8	0.65	0.40	16.99	2.53
0.0708	Step edge 3	0.43	0.13	1.79	2.68
0.0708	Step edge 4	0.55	0.38	5.67	2.92
0.0708	Step edge 5	0.62	0.40	10.82	2.69
0.0708	Step edge 6	1.07 (*)	0.68 (*)	11.31	2.94
0.0708	Step edge 7	0.68	0.43	14.43	2.58
0.0708	Step edge 8	0.89	0.57	15.46	2.59

0.0665	Step edge 3	0.44	0.15	1.81	2.63
0.0665	Step edge 4	0.66	0.48	4.65	2.89
0.0665	Step edge 5	0.69	0.43	10.19	2.55
0.0665	Step edge 6	1.47 (*)	0.73 (*)	10.26	2.52
0.0665	Step edge 7	0.82	0.48	13.45	2.35
0.0665	Step edge 8	0.85	0.50	14.89	2.37
0.0643	Step edge 3	0.46	0.18	1.97	2.65
0.0643	Step edge 4	0.75	0.52	4.47	2.79
0.0643	Step edge 5	0.74	0.49	9.37	2.65
0.0643	Step edge 6	1.55 (*)	0.77 (*)	9.92	2.79
0.0643	Step edge 7	0.85	0.54	12.51	2.55
0.0643	Step edge 8	0.67	0.44	14.44	2.69
0.058	Step edge 3	0.51	0.24	2.22	2.58
0.058	Step edge 4	0.88	0.60	5.62	2.86
0.058	Step edge 5	0.82	0.52	9.00	2.55
0.058	Step edge 6	1.62 (*)	0.78 (*)	9.81	2.79
0.058	Step edge 7	0.81	0.51	12.06	2.48
0.058	Step edge 8	0.73	0.48	13.51	2.62
0.0519	Step edge 3	0.62	0.38	3.53	2.62
0.0519	Step edge 4	1.08	0.64	6.33	2.58
0.0519	Step edge 5	0.77	0.49	8.88	2.55
0.0519	Step edge 6	1.21 (*)	0.74 (*)	8.49	3.14
0.0519	Step edge 7	0.81	0.49	11.18	2.43
0.0519	Step edge 8	1.00 (*)	0.65 (*)	11.77	2.83
0.046	Step edge 3	0.56	0.36	3.24	2.78
0.046	Step edge 4	0.89	0.59	6.97	2.72
0.046	Step edge 5	0.72	0.48	9.22	2.65
0.046	Step edge 6	1.05 (*)	0.63 (*)	9.06	2.61
0.046	Step edge 7	0.72	0.48	10.14	2.65
0.046	Step edge 8	1.14 (*)	0.68 (*)	9.63	2.77

Notes : Column (2) : the first step edge is located at the downstream end of the broad-crest; $U_w = q_w/d$;
 (*) deflected nappe.

Tableau I-2 - Double-tip conductivity data (Series 2)

Q_w m ³ /s (1)	Location (2)	$\frac{Y_{90}}{d_c}$ (3)	C_{mean} (4)	$\frac{(F_{ab})_{max} * d_c}{V_c}$ (5)	$\frac{U_w}{V_c}$ (6)	$\frac{V_{90}}{V_c}$ (7)	$a_{mean} * d_c$ (8)
<u>Series 2</u>							
0.1819	Step edge 6	0.51	0.23	7.70	2.55	2.63	3.6
0.1819	between step edges 6 & 7	0.50	0.31	9.92	2.89	2.73	8.1
0.1819	Step edge 7	0.47	0.23	13.60	2.77	2.79	9.1
0.1819	between step edges 7 et 8	0.60	0.40	15.19	2.77	2.73	16.4
0.1819	Step edge 8	0.59	0.38	16.37	2.75	2.85	15.7
0.1142	Step edge 5	0.45	0.26	11.20	2.98	2.84	6.6
0.1142	Step edge 6	0.65	0.50	18.55	3.05	2.86	16.3
0.1142	Step edge 7	0.59	0.43	27.38	2.96	3.00	24.7
0.1142	between step edges 7 et 8	0.64	0.53	21.68	3.32	2.88	26.1
0.1142	Step edge 8	0.54	0.43	29.94	3.23	2.99	29.2
0.058	Step edge 3	0.46	0.20	4.06	2.73	2.65	1.5
0.058	Step edge 4	0.85	0.63	10.43	3.17	2.74	6.7
0.058	Step edge 5	0.78	0.56	13.74	2.91	2.30	13.9
0.058	Step edge 6	1.24 (*)	0.76 (*)	16.45	3.40	2.75	12.1
0.058	Step edge 7	0.79	0.55	19.64	2.86	3.48	17.3

Notes : Column (2) : the first step edge is located at the downstream end of the broad-crest; $U_w = q_w/d$; (*) deflected nappe; a_{mean} : depth-averaged specific interface area.

Appendix II - Modelling cavity ejection processes (by H. CHANSON)

In skimming flows, recirculating vortices develop in the step cavities and they are maintained through the transmission of shear stress from the mainstream and by unsteady momentum exchanges between the main stream and cavity flows. At irregular time intervals, some cavity volume flows outwards and is replaced by fresh fluid (Fig. 3-3). The duration of the cavity ejection (or burst) is relatively short compared to the average ejection period. The ejections and inflows occur predominantly in the downstream region of the cavity ⁽⁹⁾. Several researchers suggested that the initiating mechanisms of the ejections resides within the fully-developed flow and not in the cavity flow itself, the ejection process being caused by interactions between low-speed streaks and vorticity structures next to the pseudo-bottom formed by the step edges (DJENEDI et al. 1994, ELAVARASAN et al. 1995).

An early cavity ejection model

ETHEMBABAOGLU (1978) developed a model of hydrodynamic instability in the free-shear layer. Vortices form in the shear layer. They are convected downstream, interacting with the downstream edge of the cavity and inducing disturbances which are in turn transmitted to the origin of the shear layer. The process generate self-induced disturbances.

The frequency of instability ⁽¹⁰⁾ may be estimated analytically. For a triangular cavity, it yields :

$$\frac{F_{ej} * (h * \cos\alpha)}{V} = 0.5 * \left(i + \frac{1}{4}\right) * \sin\alpha * \cos\alpha \quad (II-1)$$

where V is the mainstream velocity, $h * \cos\alpha$ is the cavity depth, and i is an integer. For ratios of cavity length to cavity depth L_{cav}/k_s less than 2, Equation (II-1) was close to ETHEMBABAOGLU's observations using $i = 1$ and 2. For greater cavity length ratios, $i = 2$ and 3 gave better agreement.

⁹Stepped chute data : Present study. Strip roughness data : DJENEDI et al. (1994), ELAVARASAN et al. (1995).

¹⁰which is basically the frequency of fluid ejections.

Energy considerations

Considering a skimming flow, it is hypothesised that all the energy losses occur by viscous dissipation in the cavity, with some energy exchange between the main flow and the recirculation by irregular fluid ejections. Considering the flow region located between two adjacent step edges (Fig. II-1), and during an average ejection period ΔT ⁽¹¹⁾, the continuity equation for the cavity implies :

$$Q_{out} * \Delta t = Q_{in} * \Delta t = V_{ej} \quad (II-2a)$$

where Q_{in} and Q_{out} are the inflow and outflow rates respectively, V_{ej} is the volume of ejected fluid, Δt is the ejection ⁽¹²⁾ duration. Dividing by the ejection period ΔT , Equation (II-2) may be rewritten :

$$Q_{out} * \frac{\Delta t}{\Delta T} = V_{ej} * F_{ej} \quad (II-2b)$$

where $F_{ej} = 1/\Delta T$ is the fluid ejection frequency.

At uniform equilibrium, the rate of energy loss between two adjacent step edges equals $\rho * Q * h$, where ρ is the fluid density, Q is the flow rate and h is the vertical step height. The energy is dissipated in the recirculation cavity at a rate $\rho * V_{ej} * F_{ej} * \Delta T / \Delta t * (V^2 / (2 * g) - V_{out}^2 / (2 * g))$, where V_{out} is the outflow velocity, and the inflow velocity is assumed to be equal to the flow velocity V . The energy principle yields a relationship between the dimensionless fluid ejection frequency and rate of energy loss:

$$\frac{F_{ej} * (h * \cos\alpha)}{V} = \frac{2 * W * h^2 * \cos\alpha * \frac{\Delta t}{\Delta T}}{V_{ej} * \frac{V^2}{g * d} * \left(1 - \frac{V_{out}^2}{V^2}\right)} \quad (II-3a)$$

where W is the chute width. For a wide channel with flat horizontal steps, it becomes :

$$\frac{F_{ej} * (h * \cos\alpha)}{V} = \frac{f * \frac{\Delta t}{\Delta T}}{2 * \lambda * \left(1 - \frac{V_{out}^2}{V^2}\right)} \quad \text{Flat horizontal steps (II-3b)}$$

where f is the dimensionless pseudo-bed shear stress, or Darcy friction factor, and λ is the ratio of the

¹¹The calculations are developed for an incompressible flow. Note that $\Delta T = 1/F_{ej}$ where F_{ej} is the fluid ejection frequency.

¹²A fluid ejection is sometimes called a burst or bursting event.

average fluid ejection volume V_{ej} to the total cavity volume.

Discussion

A lower limit of the average ejection frequency is set for $V_{out}/V \ll 1$ and by assuming that the ejection volume equals the cavity volume. For flat horizontal steps, it yields :

$$\left(\frac{F_{ej} * (h * \cos\alpha)}{V} \right)_{\min} = \frac{f}{2} * \frac{\Delta t}{\Delta T} \quad \text{Flat horizontal steps (II-4)}$$

The duration of fluid ejection Δt must be less than the average ejection period ΔT . Combining with the continuity equation for the cavity, it yields an upper limit of the average ejection frequency :

$$\left(\frac{F_{ej} * (h * \cos\alpha)}{V} \right)_{\max} = \frac{\frac{\Delta t}{\Delta T}}{\lambda * \left(1 + \frac{V}{V_{out}} \right)} \quad \text{Flat horizontal steps (II-5)}$$

Equations (II-3), (II-4) and (II-5) are shown in Figure II-2. Calculations were performed for $f = 0.2$, $\lambda = 0.5$, and $\Delta T/\Delta t = 7$. (Flow visualisations in stepped chute models (e.g. Present study) suggest a typical value of $\lambda = 0.5$ while visualisations of d-type cavity flows showed a ratio of average ejection period to ejection duration of about 5.5 to 8 (Table II-1).) Assuming that all energy losses take place by viscous dissipation in the recirculation cavity, the analytical solution must satisfy :

$$\left(\frac{F_{ej} * (h * \cos\alpha)}{V} \right)_{\min} \leq \frac{F_{ej} * (h * \cos\alpha)}{V} \leq \left(\frac{F_{ej} * (h * \cos\alpha)}{V} \right)_{\max} \quad \text{(II-6)}$$

Using Equations (II-3), (II-4) and (II-5), it yields that the ratio of outflow velocity to inflow velocity is centered around 0.5 :

$$\frac{1}{2} * (1 - \sqrt{1-f}) < \frac{V_{out}}{V} < \frac{1}{2} * (1 + \sqrt{1-f}) \quad \text{(II-7)}$$

A further conditions is $f \leq 1$.

Fig. II-1 - Sketch of a cavity ejection

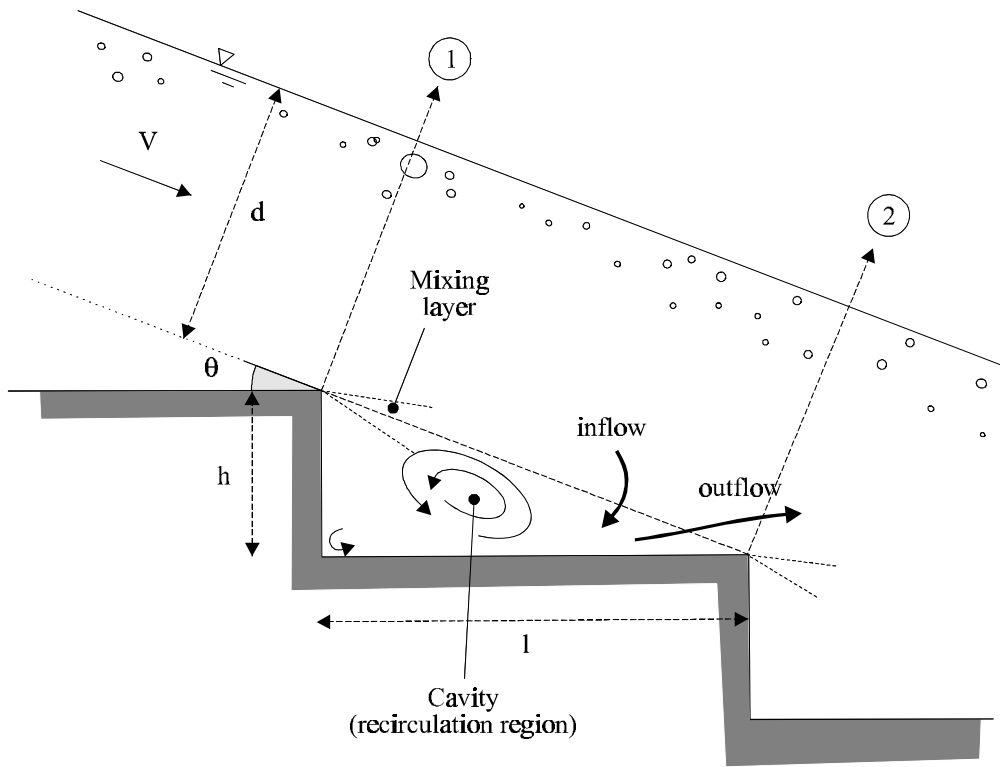


Fig. II-2 - Dimensionless average ejection frequency

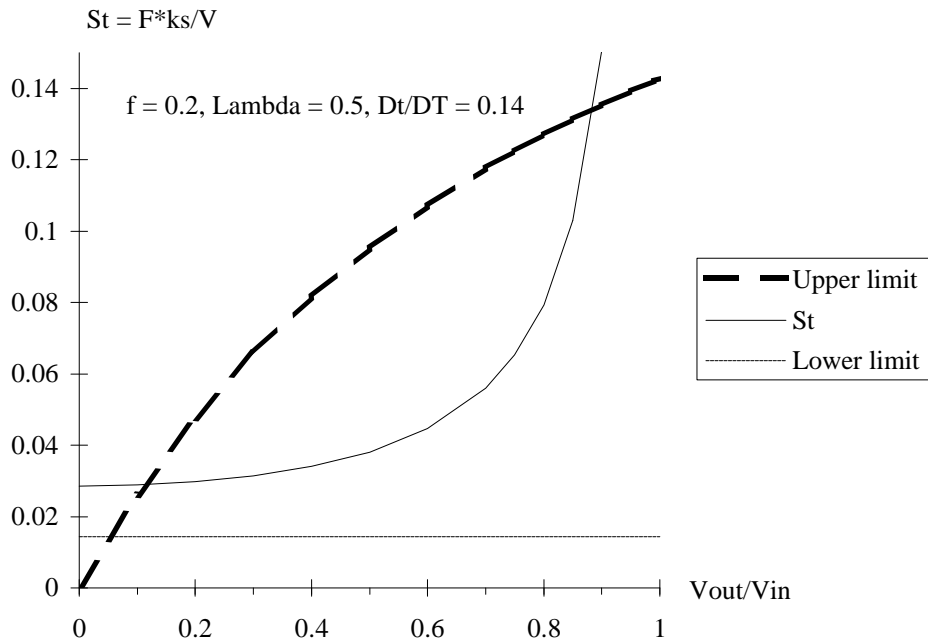


Table II-1 - Experimental observations of cavity ejections

Reference	Average ejection frequency	Ejection duration	Comments
(1)	$\frac{F_{ej} * k_s}{V_o}$	$\frac{k_s}{V_o * \Delta t}$	(4)
<u>Fully-developed flows</u>			
HEIDRICK et al. (1977)	$1.25E-3 * f * \frac{V_o * k_s}{v}$	--	Smooth pipe water flows ($\varnothing = 0.0787$ m). Fully-developed flows. $V_o = 0.4$ to 2.6 m/s.
<u>Boundary layer flows</u>			
TOWNES and SABERSKY (1966)	$0.062 * \frac{k_s * V_o}{v}$	--	Water tunnel ($W = 0.851$ m). $V_o = 0.04$ to 0.25 m/s. Square cavities : $k_s = 0.0032$ to 0.0254 m.
ETHEMBABAOGLU (1978)	0.3 to 0.58	--	Water tunnel ($d = 0.1$ m, $W = 0.24$ m). $V_o = 5.5$ to 7.5 m/s, $\delta_{BL} = 0.036$ m, $\delta_* = 0.0042$ m. Single rectangular cavities : $k_s = 0.1$ m, $L_{cav}/k_s = 1.9$ to 3.6 .
BANDYOPDHAY (1987)	$\sim 1.2 * \frac{k_s * V_o}{v}$	--	Wind tunnel ($d = 0.18$ m, $W = 0.28$ m). $V_o < 40$ m/s. Rectangular cavities : $k_s = 0.003$ m, $L_{cav}/k_s = 0.7$ to 3.0 .
DJENEDI et al. (1994)	$0.182 * \frac{k_s}{\delta_{BL}}$	$\frac{k_s}{\delta_{BL}}$	Water tunnel ($d = 0.26$ m, $W = 0.26$ m). $V_o = 0.4$ m/s, $\delta_{BL} = 0.035$ m, $\delta_M = 0.0025$ m. Square cavities : $k_s = 5$ mm.
TANTIRIDGE et al. (1994)	0.017	0.138	Square tunnel ($d = 0.025$ m, $W = 0.025$ m). Fully-developed inflow. $V_o = 0.43$ m/s. Triangular cavity : $k_s = 1.5$ mm, $\alpha = 45^\circ$.
<u>Open channel flows</u>			
SUMER et al. (2001)	0.05	0.3	Open channel flow ($d = 0.4$ m, $V \sim 0.4$ m/s) over large stones ($k_s = 0.0385$ m).

Notes : d : channel height or flow depth; F_{ej} : average ejection frequency; k_s : cavity depth (or roughness height); L_{cav} : cavity length; V_o : free-stream velocity; δ_{BL} : boundary layer thickness; δ_* : displacement thickness; δ_M : momentum thickness; Δt : ejection (burst) duration.

Appendix III - Air bubble diffusion in self-aerated flows (by H. CHANSON)

In supercritical flows, free-surface aeration is often observed. The phenomenon, called 'white waters', occurs when turbulence acting next to the free-surface is large enough to overcome both surface tension for the entrainment of air bubbles and buoyancy to carry downwards the bubbles. Assuming a homogeneous air-water mixture for $C < 90\%$, the advective diffusion of air bubbles may be analytically predicted. At uniform equilibrium, the air concentration distribution is a constant with respect to the distance x in the flow direction. The continuity equation for air in the air-water flow yields :

$$\frac{\partial}{\partial y} \left(D_t * \frac{\partial C}{\partial y} \right) = \cos \alpha * \frac{\partial}{\partial y} (u_r * C) \quad (\text{III-1})$$

where D_t is the turbulent diffusivity, u_r is the bubble rise velocity, α is the channel slope and y is measured perpendicular to the mean flow direction. The bubble rise velocity in a fluid of density $\rho_w * (1-C)$ equals :

$$u_r^2 = [(u_r)_{\text{Hyd}}]^2 * (1 - C) \quad (\text{III-2})$$

where $(u_r)_{\text{Hyd}}$ is the rise velocity in hydrostatic pressure gradient (CHANSON 1995b,1997b). A first integration of the continuity equation for air in the equilibrium flow region leads to :

$$\frac{\partial C}{\partial y'} = \frac{1}{D'} * C * \sqrt{1 - C} \quad (\text{III-3})$$

where $y' = y/Y_{90}$ and $D' = D_t / (u_r)_{\text{Hyd}} * \cos \alpha * Y_{90}$ is a dimensionless turbulent diffusivity. D' is the ratio of the air bubble diffusion coefficient to the rise velocity component normal to the flow direction times the characteristic transverse dimension of the shear flow.

Assuming a homogeneous turbulence across the flow (i.e. D' constant), it yields :

$$C = 1 - \tanh^2 \left(K' - \frac{y'}{2 * D'} \right) \quad (\text{III-4})$$

where \tanh is the hyperbolic tangent function and K' a dimensionless integration constant (CHANSON 1995b,1997b). A relationship between D' and K' is deduced for $C = 0.9$ for $y' = 1$:

$$K' = K^* + \frac{1}{2 * D'} \quad (\text{III-5})$$

where $K^* = \tanh^{-1}(\sqrt{0.1}) = 0.32745015...$ The diffusivity and the mean air content C_{mean} defined in terms of Y_{90} are related by :

$$C_{\text{mean}} = 2 * D' * \left(\tanh \left(K^* + \frac{1}{2 * D'} \right) - \tanh(K^*) \right) \quad (\text{III-6})$$

Advanced void fraction distribution models may be developed assuming a non constant diffusivity. Results are shown in Table III-1. Columns (1) and (2) show the analytical solutions of the air concentration and air bubble diffusivity distributions respectively. Column (3) lists successful applications of the solution, the reference data being listed below.

Table III-1 - Analytical solutions of Equation (III-3)

C	D'	Domain of applications	Remarks
(1)	(2)	(3)	(4)
$0.9 * \sqrt{\frac{y}{Y_{90}}}$	$\frac{2}{0.9^2} * C^2 * \sqrt{1 - C}$	Transition flow (a)	$C_{\text{mean}} = 0.60.$
$K''' * \left(1 - \exp\left(-\lambda * \frac{y}{Y_{90}}\right)\right)$	$\frac{C * \sqrt{1 - C}}{\lambda * (K''' - C)}$	Transition flow (a)	$K''' = \frac{0.9}{1 - \exp(-\lambda)}$ $C_{\text{mean}} = K''' - \frac{0.9}{\lambda}$ Note : $C_{\text{mean}} > 0.45$
$1 - \tanh^2\left(K' - \frac{y/Y_{90}}{2 * D'}\right)$	Constant	Self-aerated flow, skimming flow (a)	CHANSON (1995b,1997b) $K' = K^* + \frac{1}{2 * D'}$ $K^* = \tanh^{-1}(\sqrt{0.1}) = 0.32745015...$ $C_{\text{mean}} = 2 * D' * \left(\tanh\left(K^* + \frac{1}{2 * D'}\right) - \tanh(K^*)\right)$
$1 - \tanh^2\left(K' - \frac{(y/Y_{90})^2}{4 * \lambda}\right)$	$\frac{\lambda}{y/Y_{90}}$	Self-aerated flow	$K' = K^* + \frac{1}{4 * \lambda}$ $K^* = \tanh^{-1}(\sqrt{0.1}) = 0.32745015...$ $C_{\text{mean}} = \frac{1.7637E-3 + 0.8643 * \lambda^{1.69}}{0.09547 + \lambda^{1.69}}$
$1 - \tanh^2\left(K' - \frac{(y/Y_{90})^{n+1}}{2 * (n+1) * \lambda}\right)$	$\frac{\lambda}{(y/Y_{90})^n}$	Self-aerated flow	$K' = K^* + \frac{1}{2 * (n+1) * \lambda}$ $K^* = \tanh^{-1}(\sqrt{0.1}) = 0.32745015...$
$1 - \tanh^2\left(K' - \frac{y/Y_{90}}{2 * D_o} + \frac{\left(\frac{y}{Y_{90}} - \frac{1}{3}\right)^3}{3 * D_o}\right)$	$\frac{D_o}{1 - 2 * \left(\frac{y}{Y_{90}} - \frac{1}{3}\right)^2}$	Skimming flow (a)	$K' = K^* + \frac{1}{2 * D_o} - \frac{8}{81 * D_o}$ $K^* = \tanh^{-1}(\sqrt{0.1}) = 0.32745015...$ $C_{\text{mean}} = 0.7622 * (1.0434 - \exp(-3.614 * D_o))$

Note : (a) measured at step edges.

REFERENCE DATA : (1) Smooth-invert prototype: CAIN (1978). (2) Smooth invert laboratory: STRAUB and ANDERSON (1956), XI (1988). (3) Skimming flow (laboratory): RUFF and FRIZELL (1984), TOZZI et al. (1998), Present study. (4) Transition flow (laboratory): Present study.

Appendix IV - Velocity measurements and cross-correlation techniques for dual-tip probe measurements in gas-liquid flows

In turbulent gas-liquid flows, a velocity measurement technique is based upon the successive detection

of bubbles/droplets by two sensors : i.e., double tip optical and resistivity probes (Fig. IV-1). The technique assumes that {1} the probe sensors are aligned along a streamline, {2} the bubble/droplet characteristics are little affected by the leading tip, and {3} the bubble/impact on the trailing tip is similar to that on the leading tip. In highly turbulent gas-liquid flows, the successive detection of a bubble by each probe sensor is highly improbable, and it is common to use a cross-correlation technique (e.g. CROWE et al. 1998, pp. 309-318). The time-averaged air-water velocity is defined as:

$$V = \frac{\Delta x}{T} \quad (IV-1)$$

where Δx is the distance between probe sensors and T is the travel time for which the cross-correlation function is maximum : i.e., $R(T) = R_{\max}$ where R is the normalised cross-correlation function and R_{\max} is the maximum cross-correlation value (Fig. IV-1).

The shape of the cross-correlation function provides a further information on the turbulent velocity fluctuations (Fig. IV-2). Flat cross-correlation functions are associated with large velocity fluctuations around the mean and large turbulence intensity $Tu = u'/V$, where u' is the standard deviation of the turbulent velocity fluctuations. Thin high cross-correlation curves are characteristics of small turbulent velocity fluctuations. The information must be corrected to account for the intrinsic noise of the leading probe signal and the turbulence intensity is related to the broadening of the cross-correlation function compared to the autocorrelation function (Fig. IV-1).

The definition of the standard deviation of the velocity leads to :

$$u'^2 = \frac{V^2}{N} \sum_{i=1}^N \frac{1}{t^2} * (t - T)^2 \quad (IV-2)$$

where V is the mean velocity, N is the number of samples and t is the bubble travel time data. With an infinitely large number of data points N , an extension of the mean value theorem for definite integrals may be used as the functions $1/t^2$ and $(t-T)^2$ are positive and continuous over the interval $[i = 1, N]$ (SPIEGEL 1974). It implies that there exists at least one characteristic bubble travel time t' satisfying

$t_1 \leq t' \leq t_N$ such that :

$$\left(\frac{u'}{V}\right)^2 = \frac{1}{N} * \frac{1}{t^2} * \sum_{i=1}^N (t - T)^2 \quad (IV-3)$$

That is, the standard deviation of the velocity is proportional to the standard deviation of the bubble

travel time:

$$\frac{u'}{V} = \frac{\sigma_t}{t'} \quad (\text{IV-4})$$

Assuming that the successive detections of bubbles by the probe sensors is a true random process ⁽¹³⁾, the cross-correlation function would be a Gaussian distribution :

$$R(t) = R_{\max} * \exp\left(-\left(\frac{t - T}{\sigma_T}\right)^2\right) \quad (\text{IV-5})$$

where σ_T is the standard deviation of the cross-correlation function. Defining ΔT as a time scale satisfying : $R(T+\Delta T) = R_{\max}/2$, the standard deviation equals : $\sigma_T = \Delta T/1.175$ for a true Gaussian distribution. The standard deviation of the bubble travel time σ_t is a function of both the standard deviations of the cross-correlation and autocorrelation functions :

$$\sigma_t = \frac{\sqrt{\Delta T^2 - \Delta t^2}}{1.175} \quad (\text{IV-6})$$

where Δt is the characteristic time for which the normalised autocorrelation function equals 0.5. Assuming that $t' \sim T$ and that the bubble/droplet travel distance is a constant Δx , Equation (IV-4) implies that the turbulence intensity u'/V equals :

$$Tu = \frac{u'}{V} \approx 0.851 * \frac{\sqrt{\Delta T^2 - \Delta t^2}}{T} = Tu' \quad (\text{IV-7})$$

Tu' is a dimensionless velocity scale that is characteristic of the turbulent velocity fluctuations over the distance Δx separating the probe sensors. Although Tu' is not strictly equal to the dimensionless turbulent velocity fluctuation $Tu = u'/V$, the distributions of modified turbulence intensity Tu' provide some qualitative information on the turbulent velocity field in gas-liquid flows.

KIPPHAN (1977) developed a slightly different reasoning for two-phase mixtures such as pneumatic conveying. He obtained a result of similar form :

$$\frac{u'}{U_w} = \sqrt{\frac{\sigma_T^2 - \sigma'_t{}^2}{T^2}} \quad (\text{IV-8})$$

where U_w is the mean flow velocity, T is the mean particle travel time (e.g. on the conveyor, in the pipe) and σ'_t is the standard deviation of the autocorrelation function. It is believed however that

¹³For example, affected only by random advective dispersion of the bubbles and random velocity fluctuations over the distance separating the probe sensors.

KIPPHAN's result (Eq. (IV-8)) is an approximation (¹⁴).

Discussion

Equation (IV-7) has a wider range of application than Equation (IV-8) because it is applicable to turbulent shear flows (e.g. boundary layer flow). The modified turbulence intensity Tu' (Eq. (IV-7)) may provide both qualitative and quantitative information on the turbulent velocity field in gas-liquid flows.

The first writer's experience suggests that the standard deviation of the bubble travel time is also a function of the distance Δx between sensors. For a given bubbly flow configuration and probe sensors, the cross-correlation function broaden and the maximum cross-correlation decreases with increasing distance Δx . KIPPHAN (1977) recommended an optimum distance Δx between sensor equal to :

$$\frac{(\Delta x)_{opt}}{\delta x} \approx \frac{0.35}{Tu} \quad (IV-9)$$

where δx is the characteristic sensor size in the flow direction. Equation (IV-9) does not account however for the characteristic size of the two-phase flow structure. Table IV-1 summarises successful designs of dual-tip resistivity probes. For these designs, the "optimum" probe spacing satisfies :

$$\frac{(\Delta x)_{opt}}{\delta x} = 33.5 * V_{max}^{0.27} \quad (IV-10)$$

where V_{max} is the maximum bubbly flow velocity in m/s.

The result is further affected by an offset between the leading and trailing tips of the probe. For example, CHANSON (1995c,1997b) introduced successfully such an offset to reduce the effects of separation and wake downstream of the leading tip, reported by SENE (1984) and CHANSON (1988).

¹⁴The assumptions of $t' \sim T$ and Equation (IV-7) are not strictly correct.

Table IV-1 - Characteristic dimensions of successful dual-tip resistivity probe designs

Reference (1)	Δx m (2)	δx m (3)	$\Delta x/\delta x$ (4)	V m/s (5)	Remarques (6)
Resistivity probes					
SERIZAWA et al. (1975)	0.005	2.0E-4	25	0.5 to	Bubbly pipe flows.
CAIN (1978)	0.1016	2.0E-3	50.8	15.6 to 18.5	Prototype spillway flows (Aviemore, NZ).
LEWIS and DAVIDSON (1983)	0.0015	5.0E-4	3	0.17 to 0.68	Bubble column flows.
CHANSON (1988)	0.01	3.0E-4	33.3	7 to 17	Laboratory spillway flows
BEHNIA and GILLESPIE (1991)	0.00531	5E-4	10.6	up to 6	Bubbly pipe flows.
REVANKAR and ISHII (1992)	0.004	1.2E-4	33.3	0.1 to 1	Bubbly pipe flows.
LIU and BANKOFF (1993)	0.005	1.0E-4	50	0.4 to 1.4	Bubbly pipe flows.
CHANSON (1995c,1997b)	0.008	5.0E-5	160	1 to 9	Laboratory experiments : open channel flows, stepped cascade flows, plunging jet flows, water jets discharging into air.
Fibre optic probes					
CHABOT et al. (1992)	0.004 to 0.009	1E-3	4 to 9	0.5	Bubble column flows.

Fig. IV-1 - Sketch of a cross-correlation function and dual-tip probe

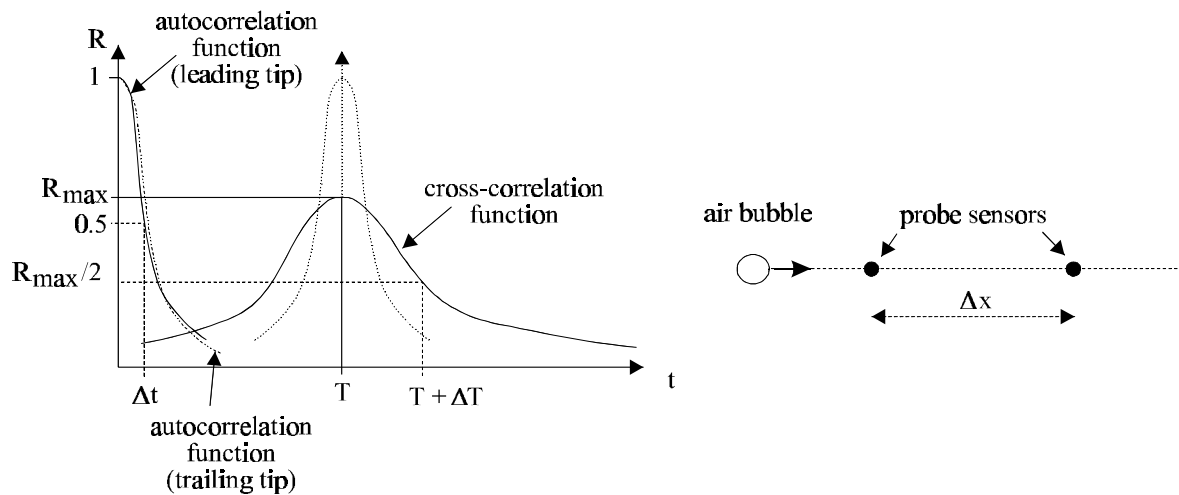
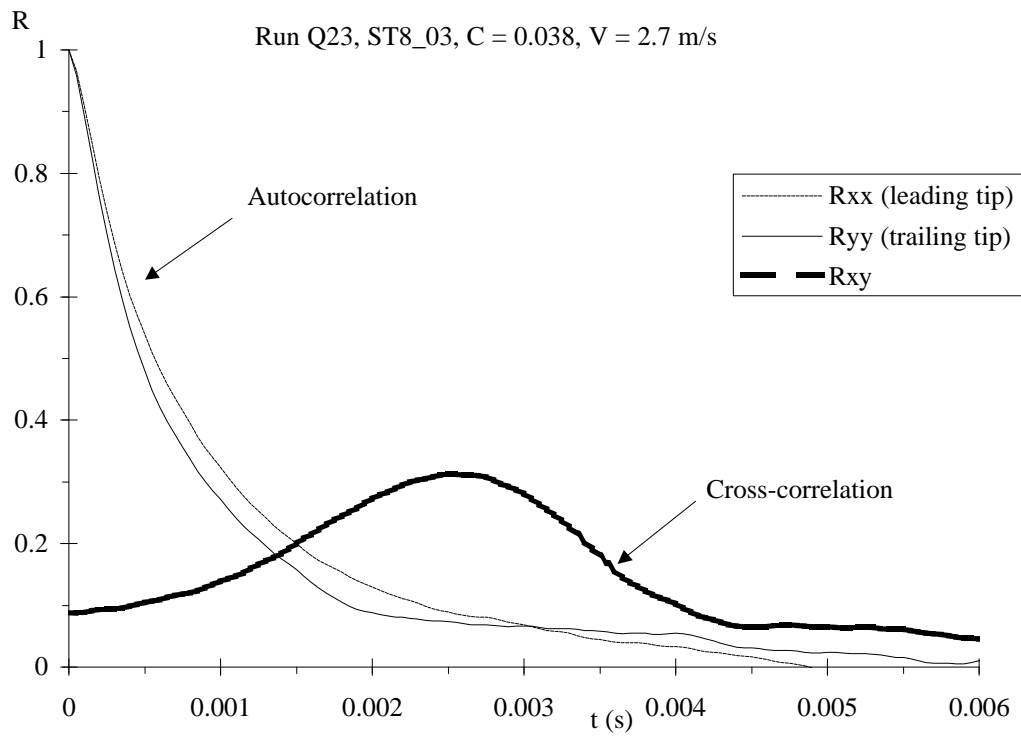


Fig. IV-2 - Examples of autocorrelation and cross-correlation functions (Run Q23)



References

- ABDUL-KHADER, M.H., and RAI, S.P. (1980). "A Study of Channel obstructions with a Longitudinal Slot." *Proc. 7th Australasian Hydraulics and Fluid Mechanics Conf.*, IEAust., Brisbane, Australia, pp. 175-178.
- ACKERS, P., WHITE, W.R., PERKINS, J.A., and HARRISON, A.J.M. (1978). "Weirs and Flumes for Flow Measurement." *John Wiley*, Chichester, UK, 327 pages.
- ANWAR, H.O. (1994). "Self-Aerated Flows on Chutes and Spillways - Discussion." *Jl of Hyd. Engrg.*, ASCE, Vol. 120, No. 6, pp. 778-779.
- AZAIEZ, J. (2000). "Reduction of Free Shear Flows Instabiity: Effects of Polymer versus Fibre Additives." *Jl of Non-Newtonian Fluid Mechanics*, Vol. 91, pp. 233-254.
- BAKER, R. (2000). "The CIRIA Guide for the Design of Stepped-Block Spillways." *Intl Workshop on Hydraulics of Stepped Spillways*, Zürich, Switzerland, H.E. MINOR & W.H. HAGER Editors, Balkema Publ., pp. 155-161.
- BANDYOPADHYAT, P.R. (1987). "Rough-Wall Turbulent Boundary Layers in the Transition Regime." *Jl of Fluid Mech.*, Vol. 180, pp. 231-266.
- BEHNIA, M., and GILLESPIE, S.J. (1991). "Void Fraction Measurement by a Computerized Double-Point Resistivity Probe." *Flow Meas. Instrum.*, Vol. 2, oct., pp. 243-247.
- BOES, R.M. (1999). "Physical Model Study on Two-Phase Cascade Flow." *Proc. 28th IAHR Congress*, Graz, Austria, Session S1, 6 pages (CD-ROM).
- BOES, R.M. (2000). "Zweiphasenstroömung und Energieumsetzung auf Grosskaskaden." *Ph.D. thesis*, VAW-ETH, Zürich, Switzerland.
- BOS, M.G. (1976). "Discharge Measurement Structures." *Publication No. 161*, Delft Hydraulic Laboratory, Delft, The Netherlands (also Publication No. 20, ILRI, Wageningen, The Netherlands).
- CAIN, P. (1978). "Measurements within Self-Aerated Flow on a Large Spillway." *Ph.D. Thesis*, Ref. 78-18, Dept. of Civil Engrg., Univ. of Canterbury, Christchurch, New Zealand.
- CHABOT, J., LEE, S.L.P., SORIA, A., and LASA, H.I. de (1992). "Interaction between Bubbles and Fibre Optic Probes in a Bubble Column." *Can. Jl of Chem. Eng.*, Vol. 70, Feb., pp. 61-68.
- CHAMANI, M.R. (2000). "Air inception in Skimming Flow regime over Stepped Spillways." *Intl Workshop on Hydraulics of Stepped Spillways*, Zürich, Switzerland, H.E. MINOR & W.H.

- HAGER Editors, Balkema Publ., pp. 61-67.
- CHAMANI, M.R., and RAJARATNAM, N. (1999). "Characteristics of Skimming Flow over Stepped Spillways." *Jl of Hyd. Engrg.*, ASCE, Vol. 125, No. 4, pp. 361-368.
- CHANSON, H. (1988). "A Study of Air Entrainment and Aeration Devices on a Spillway Model." *Ph.D. thesis*, Ref. 88-8, Dept. of Civil Engrg., University of Canterbury, New Zealand (ISSN 0110-3326).
- CHANSON, H. (1993a). "Stepped Spillway Flows and Air Entrainment." *Can. Jl of Civil Eng.*, Vol. 20, No. 3, June, pp. 422-435.
- CHANSON, H. (1993b). "Self-Aerated Flows on Chutes and Spillways." *Jl of Hyd. Engrg.*, ASCE, Vol. 119, No. 2, pp. 220-243. Discussion : Vol. 120, No. 6, pp. 778-782.
- CHANSON, H. (1994) "Drag Reduction in Open Channel Flow by Aeration and Suspended Load." *Jl of Hyd. Res.*, IAHR, Vol. 32, No. 1, pp. 87-101.
- CHANSON, H. (1995a). "Hydraulic Design of Stepped Cascades, Channels, Weirs and Spillways." *Pergamon*, Oxford, UK, Jan., 292 pages.
- CHANSON, H. (1995b). "Air Bubble Diffusion in Supercritical Open Channel Flow." *Proc. 12th Australasian Fluid Mechanics Conference AFMC*, Sydney, Australia, R.W. BILGER Ed., Vol. 2, pp. 707-710.
- CHANSON, H. (1995c). "Air Bubble Entrainment in Free-surface Turbulent Flows. Experimental Investigations." *Report CH46/95*, Dept. of Civil Engineering, University of Queensland, Australia, June, 368 pages.
- CHANSON, H. (1996). "Prediction of the Transition Nappe/Skimming Flow on a Stepped Channel." *Jl of Hyd. Res.*, IAHR, Vol. 34, No. 3, pp. 421-429.
- CHANSON, H. (1997a). "A Short History of Stepped Cascades in Australia." *ANCOLD Bulletin*, No. 106, Aug., pp. 101-111.
- CHANSON, H. (1997b). "Air Bubble Entrainment in Free-Surface Turbulent Shear Flows." *Academic Press*, London, UK, 401 pages.
- CHANSON, H. (1997c). "Measuring Air-Water Interface Area in Supercritical Open Channel Flow." *Water Res.*, IAWPRC, Vol. 31, No. 6, pp. 1414-1420.
- CHANSON, H. (1999a). "Turbulent Open-Channel Flows : Drop-Generation and Self-Aeration.

- Discussion." *Jl of Hyd. Engrg.*, ASCE, Vol. 125, No. 6, pp. 668-670.
- CHANSON, H. (1999b). "The Hydraulics of Open Channel Flows : An Introduction." *Butterworth-Heinemann*, Oxford, UK, 512 pages. (Reprinted in 2001)
- CHANSON, H. (2000). "Forum article. Hydraulics of Stepped Spillways: Current Status." *Jl of Hyd. Engrg.*, ASCE, Vol. 126, No. 9, pp. 636-637.
- CHANSON, H. (2000b). "A Review of Accidents and Failures of Stepped Spillways and Weirs." *Proc. Instn Civ. Engrs Water and Maritime Engrg*, UK, Vol. 142, Dec., pp. 177-188.
- CHANSON, H. (2001). "The Hydraulics of Stepped Chutes and Spillways." *Balkema Publ.*, Rotterdam, The Netherlands.
- CHANSON, H., and BRATTBERG, T. (1998). "Air Entrainment by Two-Dimensional Plunging Jets : the Impingement Region and the Very-Near Flow Field." *Proc. 1998 ASME Fluids Eng. Conf., FEDSM'98*, Washington DC, USA, June 21-25, Paper FEDSM98-4806, 8 pages (CD-ROM).
- CHANSON, H., and TOOMBES, L. (1997). "Flow Aeration at Stepped Cascades." *Research Report No. CE155*, Dept. of Civil Engineering, University of Queensland, Australia, June, 110 pages.
- CHANSON, H., and TOOMBES, L. (2000). "Stream Reaeration in Nonuniform Flow: Macroroughness Enhancement." *Jl of Hyd. Engrg.*, ASCE, Vol. 126, No. 3, pp. 222-224.
- CHANSON, H., YASUDA, Y., and OHTSU, I. (2000). "Flow Resistance in Skimming Flow : a Critical Review." *Intl Workshop on Hydraulics of Stepped Spillways*, Zürich, Switzerland, H.E. MINOR & W.H. HAGER Editors, Balkema Publ., pp. 95-102.
- CHANSON, H., and WHITMORE, R.L. (1998). "Gold Creek Dam and its Unusual Waste Waterway (1890-1997) : Design, Operation, Maintenance." *Can. Jl of Civil Eng.*, Vol. 25, No. 4, Aug., pp. 755-768 & Front Cover.
- COOK, N.J. (1990). "The Designer's Guide to Wind Loading of Building Structures. Part 2 : Static Structures." *Building Research Establishment & Butterworths*, London, UK, 586 pages.
- CROWE, C., SOMMERFIELD, M., and TSUJI, Y. (1998). "Multiphase Flows with Droplets and Particles." *CRC Press*, Boca Raton, USA, 471 pages.
- DJENEDI, L, ANSELMET, F., and ANTONIA, R.A. (1994). "LDA Measurements in a Turbulent Boundary Layer over a D-Type Rough Wall." *Experiments in Fluids*, Vol. 16, pp. 323-329.
- ELAVARASAN, R., PEARSON, B.R., and ANTONIA, R.E. (1995). "Visualization of Near Wall

- Region in a Turbulent Boundary Layer over Transverse Square Cavities with Different Spacing." *Proc. 12th Australasian Fluid Mech. Conf. AFMC*, Sydney, Australia, Vol. 1, pp. 485-488.
- ETHEMBABAOGLU (1978). "Some Characteristics of Unstable Flow Past Slots." *Jl of Hyd. Div.*, ASCE, Vol. 104, No. HY5, pp. 649-666.
- FRIZELL, K.H. (1992). "Hydraulics of Stepped Spillways for RCC Dams and Dam Rehabilitations. " *Proc. 3rd Specialty Conf. on Roller Compacted Concrete*, ASCE, San Diego CA, USA, pp. 423-439.
- HAUGEN, H.L., and DHANAK, A.M. (1966). "Momentum Transfer in Turbulent Separated Flow past a Rectangular Cavity." *Jl of Applied Mech.*, Trans. ASME, Sept., pp. 641-664.
- HEIDRICK, T.R., BANERJEE, S., and AZAD, R.S. (1977). "Experiments on the Structure of Turbulence in Fully Developed Pipe Flow. Part 2. A Statistical Procedure for Identifying 'Bursts' in the Wall Layers and some Characteristics of Flow during Bursting Periods." *Jl of Fluid Mech.*, Vol. 82, Pt 4, pp. 705-723.
- HORNER, M.W. (1969). "An Analysis of Flow on Cascades of Steps." *Ph.D. thesis*, Univ. of Birmingham, UK, May, 357 pages.
- KELEN, N. (1933). "Gewichtsstauauern und Massive Wehre." ('Gravity Dams and Large Weirs.') *Verlag von Julius Springer*, Berlin, Germany (in German).
- KIPPHAN, H. (1977). "Bestimmung von Transportkenngrößen bei Mehrphasenströmungen mit Hilfe *Chemie Ingenieur Technik*, Vol. 49, No. 9, pp. 695-707 (in German).
- LAALI, A.R., and MICHEL, J.M. (1984). "Air Entrainment in Ventilated Cavities : Case of the Fully Developed 'Half- Cavity'." *Jl of Fluids Eng.*, Trans. ASME, Sept., Vol. 106, p.319.
- LEWIS, D.A., and DAVIDSON, J.F. (1983). "Bubble Sizes Produced by Shear and Turbulence in a Bubble Column." *Chem. Eng. Sc.*, Vol. 38, No. 1, pp. 161-167.
- LIU, T.J., and BANKOFF, S.G. (1993). "Structure of Air-water Bubbly Flow in a Vertical Pipe - II. Void Fraction, Bubble Velocity and Bubble Size Distribution." *Intl Jl of Heat and Mass Transfer*, Vol. 36, No. 4, pp. 1061-1072.
- MATOS, J., SÁNCHEZ, M., QUINTELA, A., and DOLZ, J. (1999). "Characteristic Depth and Pressure Profiles in Skimming Flow over Stepped Spillways." *Proc. 28th IAHR Congress*, Graz, Austria, Session B14, 6 pages.

- MATOS, J. (2000). "Hydraulic Design of Stepped Spillways over RCC Dams." *Intl Workshop on Hydraulics of Stepped Spillways*, Zürich, Switzerland, H.E. MINOR & W.H. HAGER Editors, Balkema Publ., pp. 187-194.
- MICHEL, J.M. (1984). "Some Features of Water Flows with Ventilated Cavities." *Jl of Fluids Eng.*, Trans. ASME, Sept., Vol. 106, p.319.
- MICHEL, J.M., and ROWE, A. (1974). "Profils Minces Supercavitants à Arrière Tronqué." *Jl La Houille Blanche*, Bo. 3, pp. 1-43.
- NAUDASCHER, E. (1967). "From Flow Instability to Flow-Induced Excitation." *Jl of Hyd. Div.*, Proc. ASCE, Vol. 93, No. HY4, pp. 15-40.
- NAUDASCHER, E., and ROCKWELL, D. (1994). "Flow-Induced Vibrations. An Engineering Guide." *IAHR Hydraulic Structures Design Manual No. 7*, Hydraulic Design Considerations, Balkema Publ., Rotterdam, The Netherlands, 413 pages.
- OHTSU, I., and YASUDA, Y. (1997). "Characteristics of Flow Conditions on Stepped Channels." *Proc. 27th IAHR Biennial Congress*, San Francisco, USA, Theme D, pp. 583-588.
- OHTSU, I, YASUDA, Y., and TAKAHASHI, M. (2000). "Characteristics of Skimming Flow over Stepped Spillways. Discussion." *Jl of Hyd. Engrg.*, ASCE, Vol. 126, No. 11, pp. 869-871.
- OLIVIER, H. (1967). "Through and Overflow Rockfill Dams - New Design Techniques." *Proc. Instn. Civil Eng.*, March, 36, pp. 433-471. Discussion, 36, pp. 855-888.
- RAJARATNAM, N. (1990). "Skimming Flow in Stepped Spillways." *Jl of Hyd. Engrg.*, ASCE, Vol. 116, No. 4, pp. 587-591. Discussion : Vol. 118, No. 1, pp. 111-114.
- REVANKAR, S.T., and ISHII, M. (1992). "Local Interfacial Area Measurement in Bubbly Flow." *Intl Jl of Multiphase Flow*, Vol. 35, No. 4, pp. 913-925.
- RIEDIGER, S. (1989). "Influence of Drag Reducing Additives on a Plane Mixing Layer." *Proc. 4th Intl Conf. on Drag Reduction*, Davos, Switzerland, Ellis Horwood Publ., Chichester, UK, No. 10.4, pp. 303-310.
- ROUSE, H. (1937). "Modern Conceptions of the Mechanics of Turbulence." *Transactions*, ASCE, Vol. 102, pp. 463-543.
- RUFF, J.F., and FRIZELL, K.H. (1994). "Air Concentration Measurements in Highly-Turbulent Flow on a Steeply-Sloping Chute." *Proc. Hydraulic Engineering Conf.*, ASCE, Buffalo, USA, Vol. 2,

pp. 999-1003.

SCHLICHTING, H. (1979). "Boundary Layer Theory." *McGraw-Hill*, New York, USA, 7th edition.

SCHUYLER, J.D. (1909). "Reservoirs for Irrigation, Water-Power and Domestic Water Supply." *John Wiley & sons*, 2nd edition, New York, USA.

SENE, K.J. (1984). "Aspects of Bubbly Two-Phase Flow." *Ph.D. thesis*, Trinity College, Cambridge, UK, Dec..

SERIZAWA, A., KATAOKA, I., and MICHİYOSHI, I. (1975). "Turbulence Structure of Air-Water Bubbly Flows - I. Measuring Techniques." *Intl Jl Multiphase Flow*, Vol. 2, No. 3, pp. 221-233

SHVAINSHTEIN, A.M. (1999). "Stepped Spillways and Energy Dissipation." *Gidrotekhnicheskoe Stroitel'stvo*, No. 5, pp. 15-21 (in Russian). (Also *Hydrotechnical Construction*, Vol. 3, No. 5, 1999, pp. 275-282.)

SILBERMAN, E., and SONG, C.S. (1961). "Instability of Ventilated Cavities." *Jl of Ship Res.*, Vol. 5, No. 1, pp. 13-33.

SPIEGEL, M.R. (1974). "Mathematical Handbook of Formulas and Tables." *McGraw-Hill Inc.*, New York, USA.

STRAUB, L.G., and ANDERSON, A.G. (1958). "Experiments on Self-Aerated Flow in Open Channels." *Jl of Hyd. Div.*, Proc. ASCE, Vol. 84, No. HY7, paper 1890, pp. 1890-1 to 1890-35.

SUMER, B.M., COKGOR, S., and FREDSE, J. (2001). "Suction Removal of Sediment from between Armor Blocks." *Jl of Hyd. Engrg.*, ASCE, Vo. 127, No. 4, pp. 293-306.

SURYANARAYANA, G.K., PAUER, H., and MEIER, G.E.A. (1993). "Bluff-Body Drag Reduction by Passive Ventilation." *Exp. in Fluids*, Vol. 16, pp. 73-81.

SURYANARAYANA, G.K., and PRABHU, A. (2000). "Effect of natural ventilation on the boundary layer separation and near-wake vortex shedding characteristics of a sphere." *Exp. in Fluids*, Vol. 19, No. 6, pp. 582-591.

TALBOT, J.R., ROBINSON, K.M., and KADAVY, P.E. (1997). "Hydraulic Model Study of a Roller Compacted Concrete Stepped Spillway with Converging Chute Walls." *Proc. Association of State Dam Safety Officials Annual Conf.*, Pittsburg PA, USA, 10 pages.

TANTIRIGE, S.C., IRIBARNE, A.P., OJHAS, M., and TRASS, O. (1994). "The Turbulent Boundary Layer over Single V-shaped Cavities." *Intl Jl Heat Mass Transfer*, Vol. 37, pp. 2261-2271.

- TOOMBES, L., and CHANSON, H. (2000). "Air-Water Flow and Gas Transfer at Aeration Cascades: a Comparative Study of Smooth and Stepped Chutes." *Intl Workshop on Hydraulics of Stepped Spillways*, Zürich, Switzerland, H.E. MINOR & W.H. HAGER Editors, Balkema Publ., pp. 77-84.
- TOWNES, H.W., and SABERSKY, R.H. (1966). "Experiments on the Flow over a Rough Surface." *Intl JI of Heat and Mass Transfer*, Vol. 9, pp. 729-738.
- TOZZI, M.J. (1992). "Caracterização/Comportamento de Escoamentos em Vertedouros com Paramento em Degraus." ('Hydraulics of Stepped Spillways.') *Ph.D. thesis*, University of Sao Paulo, Brazil (in Portuguese).
- TOZZI, M., TANIGUCHI, E., and OTA, J. (1998). "Air Concentration in Flows over Stepped Spillways." *Proc. 1998 ASME Fluids Eng. Conf., FEDSM'98*, Washington DC, USA, June 21-25, Paper FEDSM98-5053, 7 pages (CD-ROM).
- TURNBULL, J.D., and McKAY, G.R. (1974). "The Design and Construction of Chinchilla Weir - Condamine River Queensland." *Proc. 5th Australasian Conf. on Hydraulics and Fluid Mechanics*, Christchurch, New Zealand, Vol. II, pp. 1-8.
- VERRON, J., and MICHEL, J.M. (1984). "Base-vented Hydrofoils of Finite Span under a Free Surface : an Experimental Investigation." *Jl of Ship Res.*, Vol. 28, No. 2, pp. 90-106.
- WEGMANN, E. (1907). "The Design of the New Croton Dam." *Transactions*, ASCE, Vol. LXVIII, No. 1047, pp. 398-457.
- WEGMANN, E. (1911). "The Design and Construction of Dams." *John Wiley & Sons*, New York, USA, 6th edition.
- WOOD, C.J. (1964). "The Effect of Base Bleed on periodic Wake." *Jl Roy. Aeronautical Soc.*, Vol. 68, pp. 477-482.
- WOOD, I.R. (1983). "Uniform Region of Self-Aerated Flow." *Jl Hyd. Eng.*, ASCE, Vol. 109, No. 3, pp. 447-461.
- WOOD, I.R. (1985). "Air Water Flows." *Proc. 21st IAHR Congress*, Melbourne, Australia, Keynote address, pp. 18-29.
- WOOD, I.R. (1991). "Air Entrainment in Free-Surface Flows." *IAHR Hydraulic Structures Design Manual No. 4*, Hydraulic Design Considerations, Balkema Publ., Rotterdam, The Netherlands, 149 pages.

XI, Ruze (1988). "Characteristics of Self-Aerated Flow on Steep Chutes." *Proc. Intl Symp. on Hydraulics for High Dams*, IAHR, Beijing, China, pp. 68-75.

YASUDA, Y., and OHTSU, I. (1999). "Flow Resistance of Skimming Flow in Stepped Channels." *Proc. 28th IAHR Congress*, Graz, Austria, Session B14, 6 pages (CD-ROM).

YASUDA, Y., and OHTSU, I. (2000). "Characteristics of Plunging Flows in Stepped Channel Chutes." *Intl Workshop on Hydraulics of Stepped Spillways*, Zürich, Switzerland, H.E. MINOR & W.H. HAGER Editors, Balkema Publ., pp. 147-152.

Internet Resources

Overflow embankment stepped spillways. Earth dam spillways with precast concrete blocks	http://www.uq.edu.au/~e2hchans/over_st.html
The Minimum Energy Loss (MEL) weir design. An overflow earthfill embankment dam	http://www.uq.edu.au/~e2hchans/mel_weir.html
Self-aeration on chute and stepped spillways - Air entrainment and flow aeration in open channel flows	http://www.uq.edu.au/~e2hchans/self_aer.html
Timber Crib Weirs in Queensland, Australia	http://www.uq.edu.au/~e2hchans/tim_weir.html
Current expertise and experience on stepped channel flows	http://www.uq.edu.au/~e2hchans/dpri/topic_2.html

The bibliographic reference of the present report is :

CHANSON, H., and TOOMBES, L. (2001). "Experimental Investigations of Air Entrainment in Transition and Skimming Flows down a Stepped Chute. Application to Embankment Overflow Stepped Spillways." *Research Report No. CE158*, Dept. of Civil Engineering, The University of Queensland, Brisbane, Australia, July (ISBN 1 864995297).

The Research Report CE158 is available, in the present form, as a .PDF file on the Internet at the following address :

http://www.uq.edu.au/~e2hchans/reprints/ce158.pdf
